International Journal of Engineering Research and Development
e- ISSN: 2278-067X, p-ISSN: 2278-800X, www.ijerd.com
Volume 22, Issue 9 (September 2026), PP 147-153

Effect of Carburization on TiC Precipitation Hardening and Microstructural Development in Mo–Ti Alloys

[1]Sujita Sujita, [1]Rudy Sutanto
[1]*Department of Mechanical Engineering, Faculty of Engineering*
University of Mataram, Mataram, West Nusa Tenggara, INDONESIA
Corresponding Author: Sujita Sujita.

ABSTRACT
This report provides a comprehensive review of the microstructural development and hardening mechanisms in Molybdenum-Titanium (Mo-Ti) alloys subjected to carburization and subsequent heat treatments. Molybdenum alloys are critical for high-temperature structural applications, however, their utility is often limited by surface wear and low-temperature brittleness. Carburization has emerged as a robust method for surface and internal strengthening through the precipitation of Titanium Carbide (TiC).Evidence suggests that carburization leads to the formation of finely dispersed TiC precipitates, which significantly enhance hardness—often by over 400% in pure titanium systems and providing substantial increases in Mo-Ti alloys. The report details the evolution of microstructures, including the transition from plate-like to cellular subgrain structures, and explores the synergy between precipitation hardening, solution strengthening, and grain refinement. While significant progress has been made in understanding these systems, gaps remain regarding the long-term stability of nano-carbides under extreme conditions and the optimization of additive manufacturing processes for these complex alloys.

Key Words: *Carburization, Mo–Ti Alloys, TiC Precipitation, Precipitation Hardening, Microstructural Evolution, Carbon Diffusion.*

Date of Submission: 10-09-2026 Date of acceptance: 20-09-2026

I. INTRODUCTION

Molybdenum (Mo)-based alloys are attractive for aerospace, nuclear, and other high-temperature applications because of their high melting temperature, good thermal conductivity, low coefficient of thermal expansion, and ability to retain mechanical strength at elevated temperatures. However, the practical application of Mo-based materials is constrained by their susceptibility to low-temperature recrystallization embrittlement and inadequate oxidation resistance. Consequently, alloying and microstructural engineering have been widely investigated to improve their mechanical and high-temperature performance. In particular, the incorporation of titanium (Ti), together with carbon and other refractory alloying elements, has been employed to promote strengthening through the formation and stabilisation of carbide phases and to refine the microstructure of Mo-based alloys [6], [8], [13].

The Mo–Ti system is of particular interest because Ti has a strong affinity for carbon and can participate in the formation of Ti-containing carbide precipitates. In Mo-based refractory alloys, TiC is an important strengthening phase because of its high hardness, thermal stability, and ability to act as a dispersed second phase within the metallic matrix. The beneficial influence of TiC on microstructure and mechanical properties has been demonstrated in Ti–Mo–TiC and related refractory alloy systems, where increasing TiC content can modify the matrix morphology, phase distribution, hardness, and mechanical response [4], [8], [13]. Similar precipitation and clustering phenomena involving Ti- and Mo-containing phases have also been reported in Ti–Mo steels, indicating the strong interaction between Ti, Mo, and carbon during thermochemical and thermal processing [5], [7]. Carbon addition is therefore an important approach for controlling carbide formation in Ti-containing alloys. Carburization provides a means of introducing carbon into a metallic substrate through a controlled high-temperature treatment, potentially promoting the formation of a hard carbide-enriched region. Previous studies on titanium and Ti-based alloys have demonstrated that gas carburization and plasma-assisted carburization can modify surface composition, generate titanium carbide-containing layers, and substantially improve surface hardness and tribological performance [11], [12]. The formation of TiC has also been investigated through alternative processing routes, including powder metallurgy and laser-based processing, where the carbon supply and processing temperature strongly influence carbide formation, phase constitution, and microstructural evolution [1], [2], [3], [10].

The precipitation of TiC in a Mo–Ti alloy is governed by the availability and diffusion of carbon, the concentration of Ti, temperature, and holding time. At sufficiently high temperatures, carbon can diffuse into the alloy and react with Ti to form TiC, while subsequent growth and distribution of the carbide phase depend on the thermal history and local chemical composition. Studies of Mo-containing refractory alloys have shown that processing conditions strongly affect carbide morphology, phase distribution, grain structure, and high-temperature mechanical behaviour [6], [8], [13]. Furthermore, investigations of Ti–Mo steels have demonstrated that Mo can influence the precipitation behaviour and spatial distribution of Ti-containing phases, highlighting the importance of Mo–Ti interactions in controlling precipitation strengthening [5], [7]. These findings suggest that carburization parameters should be considered not only in terms of carbon uptake but also in relation to TiC nucleation, growth, and interaction with the Mo-rich matrix.

Despite the extensive research on TiC-containing Ti–Mo composites, Mo-based Ti-containing refractory alloys, and carburized titanium materials, the relationship between carburization conditions, TiC precipitation, and microstructural development in Mo–Ti alloys remains insufficiently clarified. In particular, the effects of carburization temperature, treatment duration, and carbon availability on the evolution of TiC precipitates and the resulting hardening response require systematic investigation. Understanding these relationships is essential for establishing a processing–microstructure–property relationship for carburized Mo–Ti alloys.

Therefore, this study investigates the effect of carburization on TiC precipitation hardening and microstructural development in Mo–Ti alloys. Particular attention is given to the influence of carburization temperature and duration on carbon incorporation, TiC formation, phase evolution, microstructural characteristics, and hardness. The results are expected to provide a basis for optimising thermochemical processing conditions and developing Mo–Ti alloys with improved surface hardness, microstructural stability, and mechanical performance for demanding high-temperature applications.

.

II. MATERIAL AND METHODS

2.1. Materials

The material Mo–Ti alloy was selected as the substrate material for the carburization treatment. Mo–Ti alloys containing 1.5 wt% Ti, designated as Ti15, respectively. The materials were produced by powder metallurgy in the form of plates with an initial thickness of 1 mm. The alloy was prepared in the form of the plates were subsequently cut into specimens measuring 50 mm in length and 5 mm in width, suitable for thermochemical treatment and subsequent microstructural and mechanical characterization. The nominal chemical composition of the Mo–Ti alloy was determined using energy-dispersive X-ray spectroscopy (EDS) and/or optical emission spectroscopy prior to carburization. Prior to heat treatment, the specimen surfaces were mechanically ground using #600 emery paper to obtain a uniform and sufficiently clean surface condition for subsequent carburization.

Teak charcoal is used as a carbon source in the carburization medium, while $BaCO_3$ is used as an activator, in a ratio of 80 (wt%) teak charcoal to 20 (wt%) $BaCO_3$. The carburizing medium was selected to provide a sufficiently high carbon activity during the high-temperature treatment. Prior to use, the carbon source was dried and homogenized to minimize variations in particle size and moisture content. The specimens and carburizing medium were placed in a sealed carburizing box to minimize uncontrolled oxidation during heat treatment.

2.3. Research Methods

To achieve an initial microstructure, the specimens were heat treated under vacuum conditions of approximately 1.3×10^{-4} Pa at 1.500 ˚C for 1 hour. Following recrystallization, carburization was performed by embedding the specimens in powdered carbon contained within carburizing box The carburization process was conducted in a laboratory electric furnace using a sealed carburizing container/carburizing box. The specimens were embedded completely in the carburizing medium and positioned such that sufficient contact between the specimen surface and carburizing medium was maintained throughout the treatment.

The treatment was conducted at 850 ˚C for three different soaking times of 1, 2, 2.5, and 3 h. This carburization treatment was intended to promote further diffusion of carbon from the carburized surface toward the interior of Mo–Ti alloy specimens. These specimens were designated as 850-1, 850-2, 850-2.5 and 850-3. For cross-sectional characterization, the heat-treated specimens were sectioned through the center and mounted in epoxy resin to facilitate metallographic preparation. The exposed cross-sections were mechanically ground using #600 emery paper and subsequently buff-polished to obtain a smooth surface suitable for microscopic examination. To improve the quality of microstructural observations, the polished cross-sections were electropolished using a methyl alcohol–sulfuric acid electrolyte with a volume ratio of $CH_3OH:H_2SO_4$ = 17:3 at an applied voltage of 15 V.

The hardness distribution was evaluated using a Vickers microhardness test to determine the variation in hardness from the carburized surface toward the interior of the specimen. A test load of 25 g with a holding time of 15 s was employed, and measurements were performed at successive positions along the thickness direction. The hardness profiles were then used to assess the depth and effectiveness of carbon-induced hardening and precipitation within the Mo–Ti alloys. Optical microscopy was employed to examine the initial and carburized microstructures, determine the average grain size, and evaluate the thickness of the carburized or hardened surface layer.

The phase constitution of the surface region was investigated by X-ray diffraction (XRD) using Cu-Kα radiation. XRD analysis was performed to identify the phases formed during carburization and to provide evidence of surface-layer formation. Transmission electron microscopy (TEM) was subsequently employed to investigate the morphology, distribution, and size of fine precipitates formed within the alloy matrix. The chemical composition of the precipitates was analyzed using energy-dispersive X-ray spectroscopy (EDX) coupled with TEM. The combined results from Vickers hardness measurements, optical microscopy, XRD, TEM, and EDX were used to establish the relationship between carburization conditions, carbon diffusion, precipitation behavior, microstructural evolution, and the resulting hardness distribution in pure Mo and Mo–Ti alloys.

III. RESULT AND DISCUSSION

3.1. Hardness Test Results for Molybdenum Alloys

The hardness profiles of the carburized Ti10 alloy provide clear evidence that carburization promotes significant hardening in the region adjacent to the surface, followed by a gradual decrease in hardness with increasing distance from the carburized boundary. As shown in Figs.1, the hardness of the untreated/recrystallized region is approximately 210–230 HV, whereas the carburized specimens exhibit substantially higher hardness, particularly within the first several tens of micrometers from the boundary. This behavior is consistent with the occurrence of internal carburization in Mo–Ti alloys, in which carbon introduced from the carburizing environment diffuses into the Mo-based matrix and preferentially interacts with Ti. Previous investigations have directly identified TiC precipitates in carburized Mo–Ti alloys and attributed the increase in hardness primarily to precipitation hardening.

The observed hardness gradient can be interpreted in terms of the carbon concentration profile generated during carburization. During exposure to powdered carbon at 850 ˚C carbon is supplied continuously to the specimen surface and subsequently transported toward the interior through solid-state diffusion. The local carbon concentration is therefore expected to be highest near the carburized boundary and progressively decrease with increasing diffusion distance. In Mo–Ti alloys, however, the effect of carbon diffusion is not governed solely by its concentration in the Mo matrix. Carbon has a strong chemical affinity for Ti, resulting in preferential Ti–C interactions and subsequent formation of TiC particles. Previous work on Mo–Ti alloys demonstrated that carbon diffusion and its interaction with Ti are central to the development of the internally carburized region.

The hardness distribution in Fig. 4 further indicates that increasing the carburization time from 1 to 3 h produces a higher hardness level over a larger subsurface region. The 850-1 condition exhibits a maximum hardness of approximately 350–370 HV near the boundary, while the 850-2 condition reaches approximately 400–420 HV in the near-surface region based on the graphical data. Beyond approximately 100–200 μm, the hardness gradually approaches the range of approximately 220–280 HV. This behavior suggests that extending the carburization time increases the amount of carbon available for diffusion and consequently increases the volume fraction of carbon-containing strengthening features within the subsurface region. Similar hardness gradients have been reported for carburized dilute Mo–Ti alloys, where hardness decreases progressively with distance from the specimen surface and the hardening inside the surface layer is associated with the interaction of Ti and C together with carbide formation.

A more pronounced hardening response is observed after the additional 3 h diffusion treatment. As shown in Fig. 5, the 850-2.5 and 850-3 conditions exhibit near-surface hardness values that can reach approximately 450–470 HV and 400–440 HV, respectively, followed by a gradual decrease toward the specimen interior. The important feature of these profiles is that the elevated hardness is not restricted to the immediate surface. Instead, relatively high hardness persists to several hundred micrometers from the boundary. This indicates that the second heat-treatment stage facilitates redistribution of carbon from the carbon-rich surface region into the Mo–Ti matrix. Thus, the two-step process can be regarded as a means of separating carbon uptake from subsequent carbon redistribution and precipitation within the alloy.

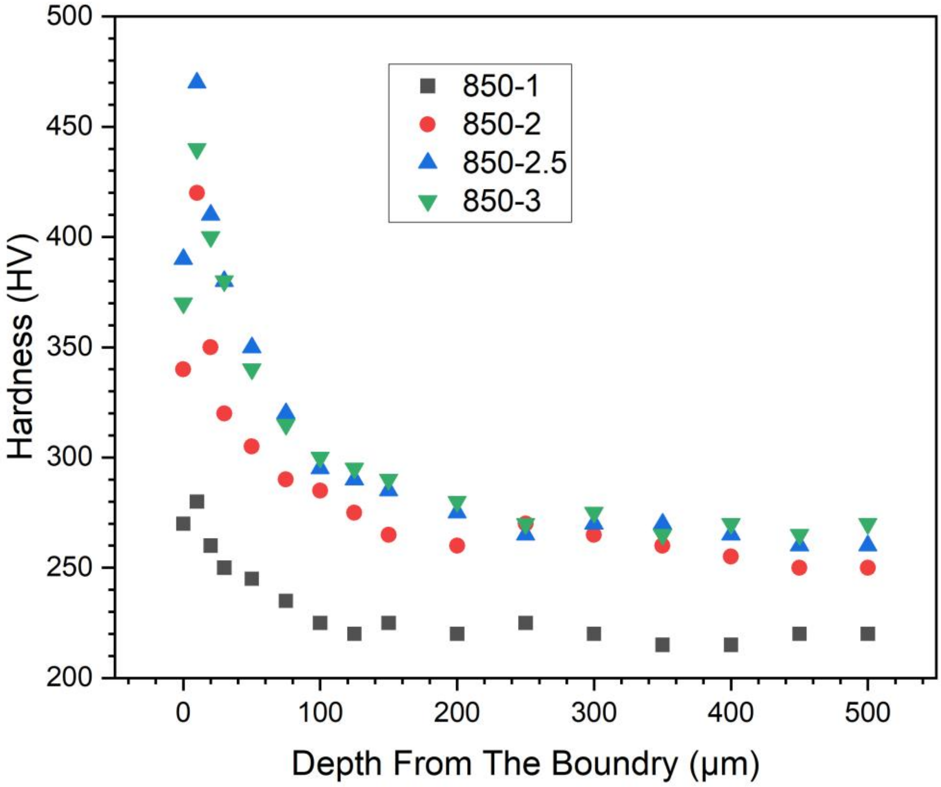

Figure 1: Hardness test results for Molybdenum alloys

The spatial correlation between hardness and diffusion distance is particularly important. Near the carburized boundary, the higher carbon availability promotes a greater density of TiC precipitates, resulting in the highest hardness. As the distance from the boundary increases, the carbon concentration decreases, reducing the amount of carbon available for TiC precipitation. Consequently, the precipitate population and associated strengthening effect are expected to decrease with depth. This provides a mechanistic explanation for the gradual reduction in Vickers hardness observed in Figs.1. Thus, the hardness profile can be considered an indirect indicator of the spatial distribution of carbon-induced precipitation strengthening, although direct quantitative correlation requires independent carbon-concentration and precipitate-density measurements.

An important distinction should also be made between solid-solution hardening and precipitation hardening. The initial Ti addition itself contributes to the hardness of the recrystallized Mo–Ti alloy through solid-solution strengthening. Previous work reported that the hardness of recrystallized Mo–Ti alloys increases approximately with increasing Ti content. After carburization, however, the additional hardening inside the surface layer cannot be explained solely by Ti in solid solution. The formation of TiC precipitates provides an additional strengthening mechanism and is considered the principal contributor to the enhanced hardness of carburized Mo–Ti alloys.

3.2. TEM Analysis of the Carburized Boundary Layer and TiC Precipitation

The TEM microstructure near the carburized boundary provides a mechanistic basis for understanding the pronounced increase in hardness observed in the near-surface region of the Ti10 alloy. As illustrated in Fig. 2(a), the region adjacent to the carburized boundary contains a relatively high population of fine second-phase particles dispersed within the Mo–Ti matrix. The distribution of these particles is considerably denser near the boundary and becomes less pronounced toward the interior. Such a spatial distribution is consistent with the carbon concentration gradient established during solid-state carburization, where carbon enters the alloy from the carbon-rich surface and subsequently diffuses toward the bulk.

The formation of the dispersed particles is closely associated with the strong chemical affinity between carbon and titanium. During carburization at elevated temperature, carbon atoms dissolve into the Mo–Ti matrix and diffuse toward regions of lower carbon concentration. Because Ti is a strong carbide-forming element, the dissolved carbon preferentially interacts with Ti atoms, resulting in the nucleation and growth of TiC precipitates. Previous experimental investigations of carburized Mo–Ti alloys using TEM and EDX confirmed the presence of TiC precipitates and attributed the increase in hardness primarily to precipitation hardening.

The high-magnification TEM representation in Fig. 2(b), illustrates a fine TiC precipitate embedded in the Mo–Ti matrix. The nanoscale dimensions of the precipitates are particularly important because fine and dispersed particles are highly effective in impeding dislocation motion. Consequently, the increase in precipitate population near the carburized boundary provides a direct microstructural explanation for the high Vickers hardness measured in this region. The strengthening contribution can be described conceptually by the interaction between mobile dislocations and nanoscale TiC particles. As the precipitate size remains small and the particles are sufficiently dispersed, dislocation movement becomes increasingly difficult, resulting in an increase in the critical stress required for plastic deformation.

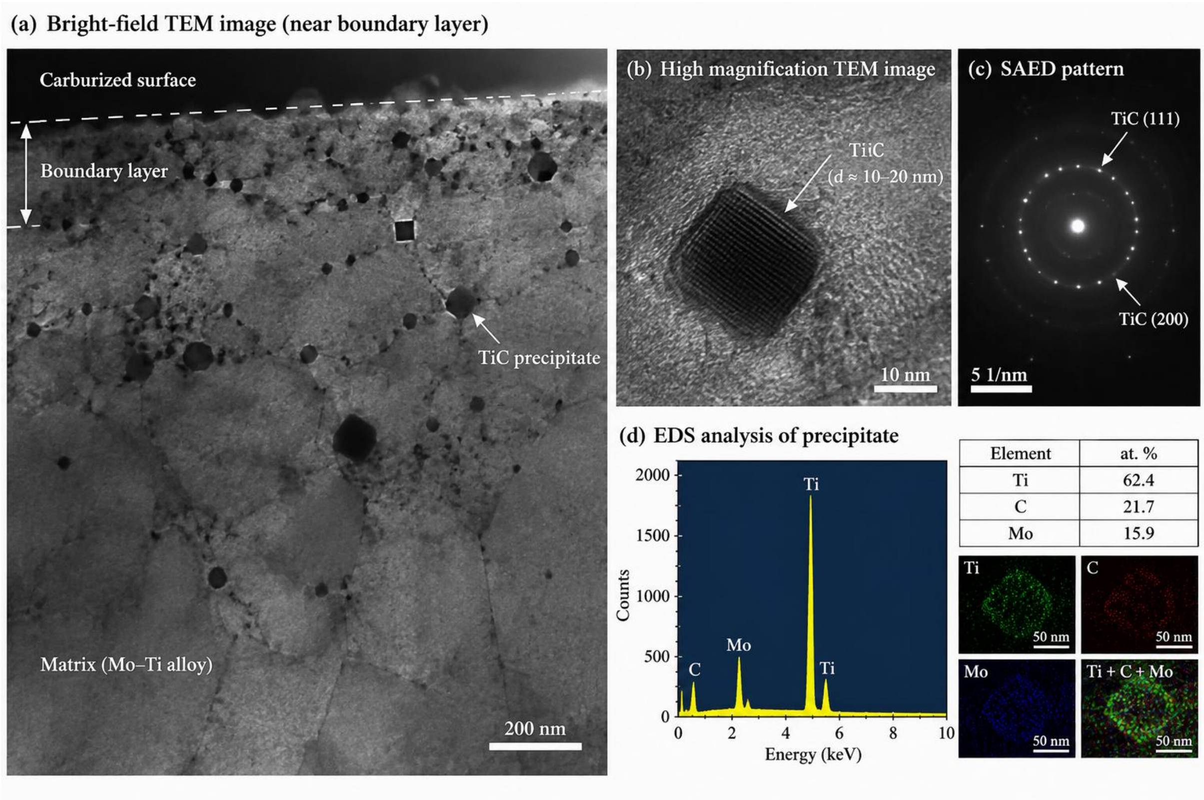

Figure 1: TEM analysis of the carburized boundary layer and TiC precipitation

The selected-area electron diffraction (SAED) pattern shown in Fig. 2(c) is consistent with the presence of a crystalline carbide phase, with reflections assigned to TiC. Together with the EDX response shown in Fig. X(d), the identification of Ti- and C-rich particles provides strong evidence for TiC formation. The simultaneous enrichment of Ti and C within the precipitate regions is particularly significant because it distinguishes carbide precipitation from simple carbon dissolution in the Mo matrix. In the context of the present carburization treatment, TiC formation can therefore be considered a principal microstructural consequence of carbon uptake by the Ti-containing Mo alloy.

The EDX elemental distribution further illustrates the spatial association between Ti and C within the precipitated particles. Regions enriched in Ti correspond closely with regions enriched in C, whereas Mo is predominantly distributed throughout the matrix. This elemental partitioning is characteristic of a precipitation process in which Ti acts as the principal carbide-forming species. The resulting TiC particles consume a portion of the carbon introduced during carburization, thereby coupling carbon diffusion with precipitation reactions. This interpretation agrees with previous work showing that carbon diffusion in Mo–Ti alloys is strongly influenced by the preferential combination between carbon and titanium.

3.2. TEM Analysis of the Carburized Boundary Layer and TiC Precipitation

The TEM observations provide an important explanation for the hardness profiles presented in Figs. 4 and 5. The hardness of the uncarburized Ti10 alloy is approximately 210–230 HV, whereas the near-boundary region after carburization exhibits substantially higher hardness. The reconstructed hardness profiles indicate values approaching approximately 350–420 HV for the 1773-3.6 and 1773-36 conditions and approximately 400–470 HV following the additional diffusion treatment. Although these values should be regarded as estimates when obtained from graphical digitization, the overall trend clearly indicates substantial subsurface hardening.

The hardness gradient can therefore be interpreted as a consequence of the spatially varying TiC precipitation density. Close to the carburized boundary, the carbon chemical potential is highest and the supply of carbon to the Ti-containing matrix is greatest. Consequently, a larger fraction of Ti can participate in carbide formation, resulting in a higher density of TiC precipitates and stronger precipitation hardening. With increasing distance from the boundary, the carbon concentration decreases because of diffusion and progressive consumption by carbide formation. The resulting lower TiC population produces a corresponding decrease in hardness.

This relationship may be expressed schematically as:

Carbon supply → carbon diffusion → Ti–C interaction → TiC nucleation → TiC growth → dislocation obstruction → hardness increase.

Thus, the hardness profile is not simply a consequence of carbon concentration alone. Instead, it reflects the combined effects of carbon diffusion, Ti–C chemical interaction, TiC precipitation, and precipitation strengthening. This distinction is important because the presence of Ti fundamentally changes the response of the Mo matrix to carburization. Previous studies reported that carburized Mo–Ti alloys develop an internally hardened region beneath the surface layer and attributed this hardening mainly to the preferential combination of Ti and C, with additional contributions from Ti in solid solution and Mo_2C.

IV. CONCLUSIONS

This study confirms that carburization effectively enhances the surface hardness of Mo–Ti alloys through the combined effects of carbon diffusion and TiC precipitation. Carbon diffuses from the surface into the alloy, producing a concentration gradient and promoting TiC formation in the carbon-enriched region. TEM observations near the carburized boundary indicate the presence of fine TiC precipitates, which act as barriers to dislocation motion and contribute to precipitation strengthening. Consequently, the highest hardness is associated with regions having higher carbon concentration and a greater density of fine TiC precipitates, while hardness gradually decreases with increasing distance from the carburized surface as carbon concentration and TiC precipitation decrease. These results demonstrate that the hardness gradient is directly related to the coupled carbon diffusion–TiC precipitation mechanism rather than carbon enrichment alone. Carburization therefore provides an effective method for developing a hardened surface while maintaining a comparatively less affected substrate. Appropriate control of carburization conditions is essential to promote fine and uniformly distributed TiC precipitates and to avoid excessive particle coarsening. Overall, the findings provide a clear basis for optimizing carburization to improve the surface mechanical and potentially tribological performance of Mo–Ti alloys.

REFERENCES

[1] Huang, K.-T., Chang, S.-H., and Wang, H.-T., "Characteristics and Properties of Ti-8Mo-6Cr Alloys with Added NbC Powders through the Vacuum Sintering Process at Various Temperatures," Materials Transactions, DOI: 10.2320/MATERTRANS.M2017128, 2017.

[2] Vrancken, B., Dadbakhsh, S., et al., "Selective Laser Melting Process Optimization of Ti-Mo-TiC Metal Matrix Composites," CIRP Annals, DOI: 10.1016/J.CIRP.2019.04.120, 2019.

[3] Wang, H., Zhang, W., Xu, Z., et al., "Synthesis of Titanium Carbide Coating on Ti15Mo Alloy and Its Tribological Behaviour," Biosurface and Biotribology, DOI: 10.1049/bsb2.12070, 2023.

[4] Wang, Z., Cheng, H., Lv, Y., et al., "Effect of TiC Content on the Microstructure and Mechanical Properties of Ti-30Mo-xTiC Composites," International Journal of Refractory Metals and Hard Materials, DOI: 10.1016/j.ijrmhm.2022.105879, 2022.

[5] Dhara, S., Marceau, R. K. W., Wood, K., et al., "Precipitation and Clustering in a Ti-Mo Steel Investigated Using Atom Probe Tomography and Small-Angle Neutron Scattering," Materials Science and Engineering A, DOI: 10.1016/J.MSEA.2018.01.070, 2018.

[6] Green, J., "Molybdenum Alloy Mo-Ti-Zr-C Adapted for Laser Powder Bed Fusion with Refined Isotropic Microstructure and Excellent High Temperature Strength," International Journal of Refractory Metals and Hard Materials, DOI: 10.1016/j.ijrmhm.2023.106174, 2023.

[7] Andrean, W. and Mayarni, "Revealing the Influence of Mo Addition on Interphase Precipitation in Ti-Bearing Low Carbon Steels," Acta Materialia, DOI: 10.1016/j.actamat.2021.117475, 2022.

[8] Uemura, S., Yamamoto Kamata, S., Yoshimi, K., et al., "Microstructural Evolution during High-Temperature Tensile Creep at 1,500°C of a MoSiBTiC Alloy," High Temperature Materials and Processes, DOI: 10.1515/HTMP-2020-0039, 2020.

[9] Gan, X., Yang, G., Zhao, G., et al., "Effect of Vanadium on the Phase Transformation Behavior of Ti-Mo Microalloyed Ultra-High Strength Steel," Steel Research International, DOI: 10.1002/SRIN.201800112, 2018.

[10] Lu, B., Zhang, C., Guo, Z., et al., "High-Carbon Ferrochrome Effects on Microstructure and Mechanical Properties of Powder Metallurgy Titanium Alloys," Journal of Materials Engineering and Performance, DOI: 10.1007/S11665-019-04282-X, 2019.

[11] Kim, H. K., Kim, H. G., et al., "Atmosphere Gas Carburizing for Improved Wear Resistance of Pure Titanium Fabricated by Additive Manufacturing," Materials Transactions, DOI: 10.2320/MATERTRANS.M2016361, 2017.

[12] Guo, L. N., Chen, J., and Pan, J. D., "Double Glow Plasma Hydrogen-Free Carburizing on the Surface of Purity Titanium," Advanced Materials Research, DOI: 10.4028/WWW.SCIENTIFIC.NET/AMR.314-316.108, 2011.

[13] Kaserer, L., Braun, J., Stajkovic, J., et al., "Microstructure and Mechanical Properties of Molybdenum-Titanium-Zirconium-Carbon Alloy TZM Processed via Laser Powder-Bed Fusion," International Journal of Refractory Metals and Hard Materials, DOI: 10.1016/J.IJRMHM.2020.105369, 2020.
[14] Li, Z., Zhao, W., Ji, S., et al., "Research Progress and Trend of Plasma Metallurgy on Titanium Metallic Surface," DOI: 10.1051/MATECCONF/202032106007, 2020.
[15] Belomyttsev, M. Yu., "A Study of Processes of Phase Formation and Hardening in Molybdenum Alloys after Internal Nitriding," Metal Science and Heat Treatment, DOI: 10.1007/S11041-018-0268-4, 2018.